79-FM-27

JSC-16064

Refraction Corrections for Surveying

Mission Planning and Analysis Division

August 1979

NASA
National Aeronautics and Space Administration

Lyndon B. Johnson Space Center
Houston, Texas

79FM27

79-FM-27

JSC-16064

SHUTTLE PROGRAM

REFRACTION CORRECTIONS FOR SURVEYING

By William M. Lear
TRW

JSC Task Monitor: Paul R. Pixley FM8
Mathematical Physics Branch

Approved: ______________________
Emil R. Schiesser, Chief
Mathematical Physics Branch

Approved: ______________________
Ronald L. Berry, Chief
Mission Planning and Analysis Division

Mission Planning and Analysis Division

National Aeronautics and Space Administration

Lyndon B. Johnson Space Center

Houston, Texas

August 1979

CONTENTS

PRECEDING PAGE BLANK NOT FILMED

TABLES

FIGURES

1.0 INTRODUCTION

Optical measurements of range and elevation angle are distorted by the Earth's atmosphere as shown in figure 1.

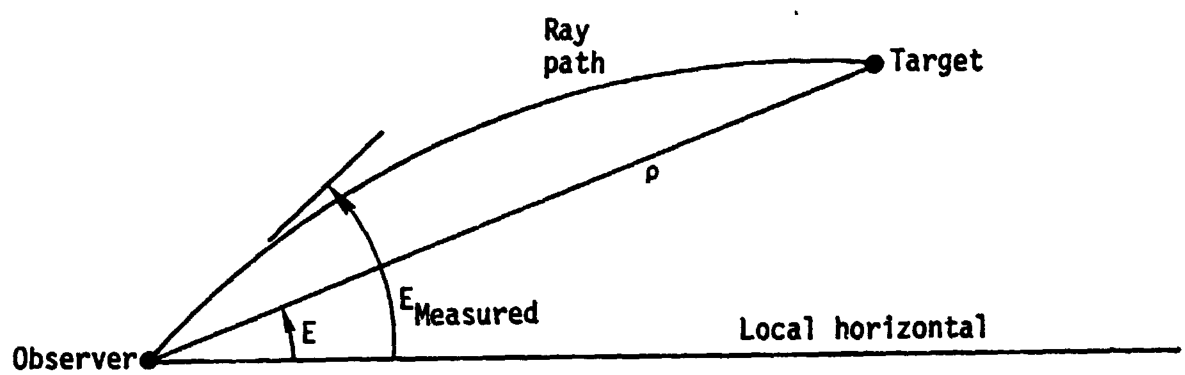

Figure 1.- Refraction effects.

For long ranges, the measured elevation angle E_M may deviate from the true elevation angle E by several milliradians, and measured range ρ_M may differ from true range ρ by several meters. Even short-range measurements are affected by refraction, and the effects are cumulative.

Intuition may lead one to think that refraction effects are minor when the elevation angle is near zero. Exactly the opposite is true. E_M-E increases with a decreasing elevation angle, and the ray path becomes more curved. Also to be noted is that a laser ranging device can not be compensated to give a true range measurement by using the speed of light in the atmosphere, at the instrument. This will not include the effects of the ray path bending and the passage through higher or lower layers of atmosphere, where the speed of light differs from that at the instrument. The equations in this report assume that measured range is obtained by using the speed of light in a vacuum (index of refraction n=1).

The work presented in this report is a spinoff of the Space Shuttle Program. The high precision refraction correction equations in this report are being used to evaluate approximate refraction correction equations developed at the NASA Johnson Space Center. It was determined that the equations in this report were ideally suited for surveying since their inputs are optically measured range and optically measured elevation angle. The outputs are true straight-line range and true geometric elevation angle. The "short" distances used in surveying allow the calculations of true range and true elevation angle to be quickly made using a programable pocket calculator.

2.0 THE SPHERICAL FORM OF SNELL'S LAW

Let n be the index of refraction. A light ray traveling from one media (n_i) to another (n_{i+1}) is bent according to Snell's law (fig. 2).

$$n_{i+1} \sin \phi_{i+1} = n_i \sin \phi_i$$

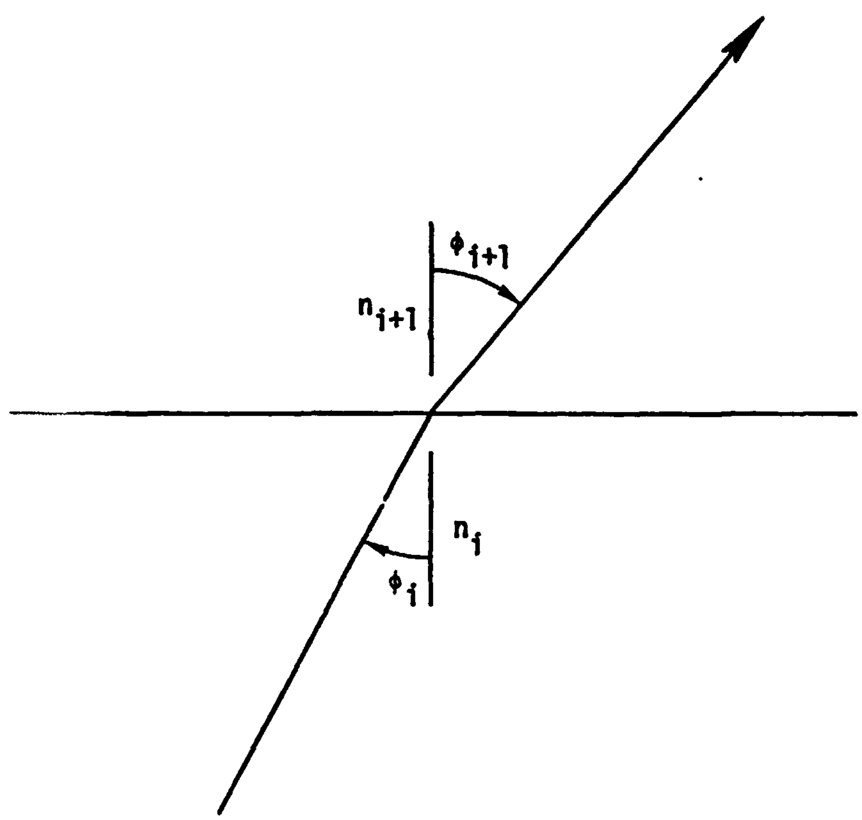

Figure 2.- Snell's law.

Figure 3 shows how Snell's law can be applicable to concentric spherical surfaces.

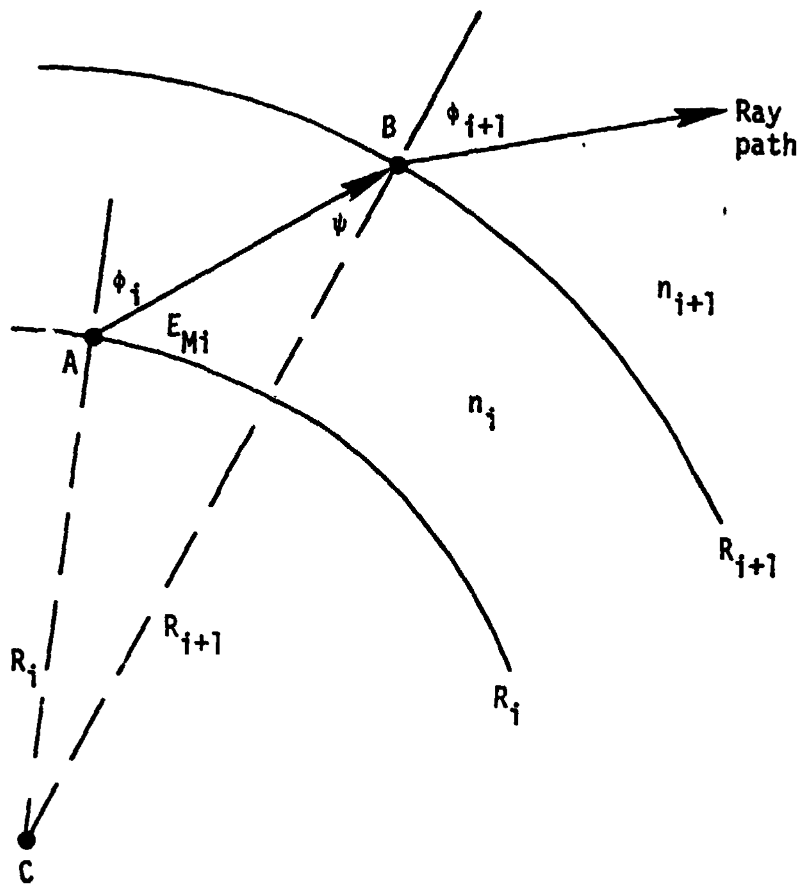

Figure 3.- Ray path across spherical surfaces.

From the ABC triangle in figure 3 and from the law of sines,

$$\frac{R_i}{\sin \psi} = \frac{R_{i+1}}{\sin(180 - \phi_i)} = \frac{R_{i+1}}{\sin \phi_i}$$

or

$$R_{i+1} \sin \psi = R_i \sin \phi_i$$

But from Snell's law of refraction,

$$\sin \psi = \frac{n_{i+1}}{n_i} \sin \phi_{i+1}$$

Thus,

$$R_{i+1} \frac{n_{i+1}}{n_i} \sin \phi_{i+1} = R_i \sin \phi_i$$

or

$$n_{i+1} R_{i+1} \sin \phi_{i+1} = n_i R_i \sin \phi_i$$

In the next layer, it is easily seen that

$$n_{i+2} R_{i+2} \sin \phi_{i+2} = n_i R_i \sin \phi_i$$

or, in general,

$$nR \sin \phi = n_i R_i \sin \phi_i$$

Elevation angle E_M is defined by

$$E_M = 90 - \phi$$

As a result, the spherical form of Snell's law is developed:

$$\boxed{nR \cos E_M = n_i R_i \cos E_{Mi}} \qquad (1)$$

The elevation angle E_M at radius R is a function only of n at R and the initial conditions: n_i, R_i, and E_{Mi}. That is, E_M is independent of the shape of the ray path (any crazy curve) from R_i to R.

3.0 THE RAY PATH EQUATIONS

Figure 4 shows the ray path geometry from the initial altitude h_i to the final altitude h_f.

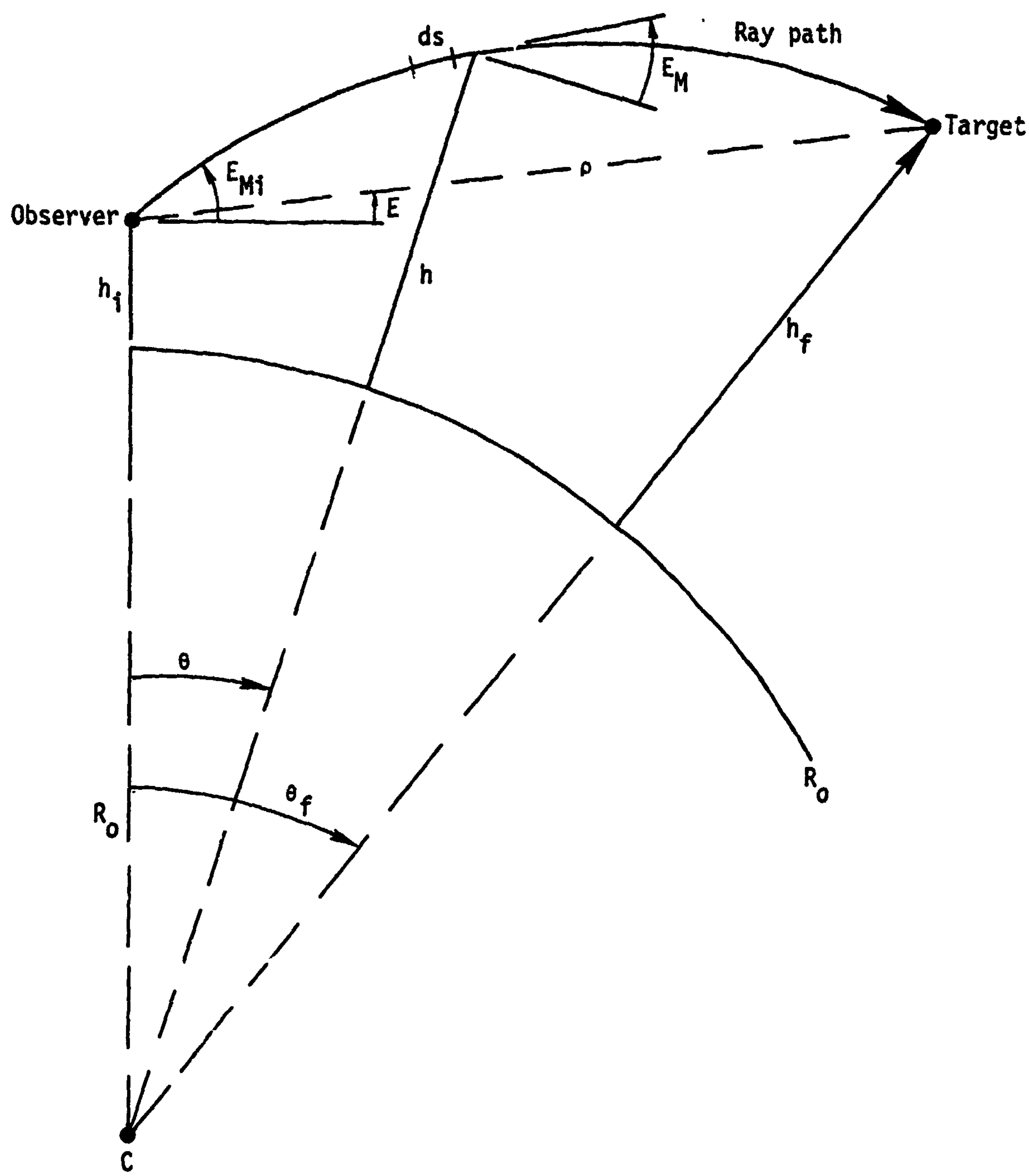

Figure 4.- Ray path geometry.

The following parameters are defined:

R_o = reference radius of Earth = 6 378 165 meters; value not critical
$R = R_o + h$

h = altitude above R_o
h_i = initial value of h
h_f = final value of h

θ = central angle
θ_i = zero
θ_f = value at target

E_M = elevation angle of ray path
E_{Mf} = value of E_M at target, final value
E_{Mi} = initial value of E_M as measured by equipment

ds = differential path length

ρ = true, straight-line, geometric range

E = true, geometric elevation angle

c = speed of light in a vacuum

n = index of refraction at h, equal to c/(speed of light at h)

n_o = value of n at R_o

ρ_M = measured range

$$\rho_M = \int n ds \tag{2}$$

The value $N = n-1$ is the modulus of refraction. An exponential atmosphere is assumed. That is,

$$N = N_o \exp(-h/H_S) \tag{3}$$

The symbol H_S is defined as atmospheric scale height.

Values of N_o and H_S are supplied by meteorologists. However, the following empirical relationship may be used for H_S (ref. 1):

$$H_S = \frac{1000}{\ln \dfrac{N_o}{N_o - 7.32 \cdot 10^{-6} \exp(5577 N_o)}} \text{ meters} \tag{4}$$

This value of H_S is used at Johnson Space Center for processing radar tracking data. However, it may not be the best for optical survey data.

Figure 5(a) shows the differential path length element ds and its two components. Figure 5(b) shows the photon velocity along ds and its two components.

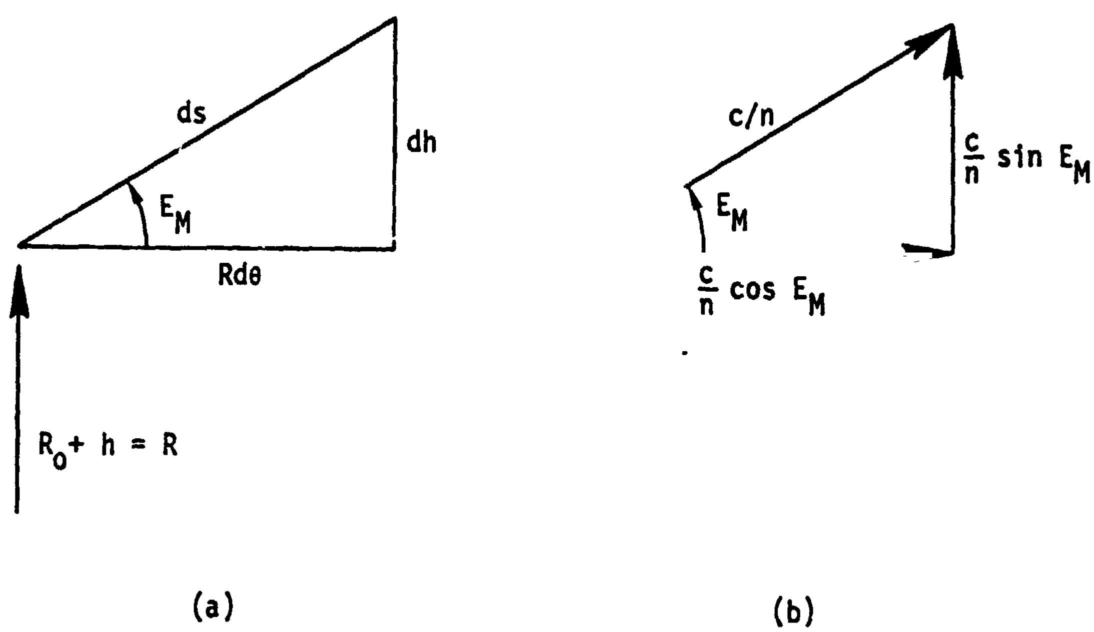

Figure 5.- Differential geometry.

Figure 5 shows that

$$\frac{ds}{dt} = \frac{c}{n} \tag{5}$$

$$\frac{dh}{dt} = \frac{c}{n} \sin E_M \tag{6}$$

$$\frac{d\theta}{dt} = \frac{1}{R}\frac{c}{n} \cos E_M \tag{7}$$

where, from equation (3), n is given as a function of h by

$$n = 1 + N = 1 + N_o \exp(-h/H_S) \tag{8}$$

Note from equation (2) that

$$d\rho_M = n\,ds$$

And, using equation (5)

$$\frac{d\rho_M}{dt} = c \tag{9}$$

An expression for E_M is now required. Equation (1), the spherical form of Snell's law of refraction, could be used; however, it is fraught with numerical problems. For example, if $E_{Mi} = 0$, then h (eq. (6)) will remain at its initial value, h_i. It has been determined that it is more accurate to develop a differential equation for E_M and integrate it. In equation (1),

$$nR \cos E_M = \text{constant}$$

Differentiating with respect to time gives

$$\dot{n}R \cos E_M + n\dot{h} \cos E_M - nR\,\dot{E}_M \sin E_M = 0$$

But, from equations (8) and (3)

$$\dot{n} = -\frac{N_o}{H_S}\,\dot{h}e^{-h/H_S} = -\frac{N}{H_S}\,\dot{h}$$

Thus,

$$-R\frac{N}{H_S}\,\dot{h} \cos E_M + n\dot{h} \cos E_M - nR\,\dot{E}_M \sin E_M = 0$$

Using equation (6) for $\dot{h}$

$$-R \frac{N}{H_S} \frac{c}{n} \sin E_M \cos E_M + c \sin E_M \cos E_M - nR \dot{E}_M \sin E_M = 0$$

And the equation for $\dot{E}_M$ is

$$\frac{dE_M}{dt} = \left(\frac{1}{R} - \frac{N}{nH_S} \right) \frac{c}{n} \cos E_M \tag{10}$$

Now, let

$$a = ct \tag{11}$$

Then $da = cdt$ and the resulting equations are summarized as follows.

$$\rho_M = a \tag{12}$$

$$\frac{dh}{da} = \frac{1}{n} \sin E_M \tag{13}$$

$$\frac{d\theta}{da} = \frac{1}{R} \frac{1}{n} \cos E_M \tag{14}$$

$$\frac{dE_M}{da} = \left(\frac{1}{R} - \frac{N}{nH_S} \right) \frac{1}{n} \cos E_M \tag{15}$$

The initial conditions are

$a = 0$

$h = h_i$

$\theta = \theta_i = 0$

$E_M = E_{Mi}$

And where

$$R = R_o + h \tag{16}$$

$$N = N_o \exp(-h/H_S) \tag{17}$$

$$n = N + 1 \tag{18}$$

The equations are integrated from $a = o$ to $a =$ measured range. All that remains is to obtain the expressions for ρ and E. It can be seen in figure 4 that

$$R_i = R_o + h_i$$

$$R_f = R_o + h_f$$

$$T_1 = R_f \cos \theta_f - R_i$$

$$T_2 = R_f \sin \theta_f$$

$$\rho = \sqrt{T_1^2 + T_2^2} \tag{19}$$

$$E = \arctan (T_1/T_2) \tag{20}$$

4.0 INTEGRATING THE EQUATIONS

A fourth order Runge-Kutta-Gill integrator has been found to be very suitable for most purposes. Other integrators may be found in reference 2. The Runge-Kutta-Gill integrator allows a maximum integration step size of about 10 000 meters for even the most precise surveying work.

Let the state vector $\underline{x}$ be defined by

$$\underline{x} = \begin{bmatrix} h \\ \theta \\ E_M \end{bmatrix} \tag{21}$$

Let

$$\underline{f}(\underline{x}) = \begin{bmatrix} dh/da \\ d\theta/da \\ dE_M/da \end{bmatrix} \tag{22}$$

Then the fourth order Runge-Kutta integrator equations (ref. 2) are:

$$\underline{x}_n = \underline{x}$$

$$\rho_M = \rho_M + \Delta a$$

$$\underline{k}_1 = \Delta a \underline{f}(\underline{x})$$

$$\underline{x} = \underline{x}_n + a_1 \underline{k}_1$$

$$\underline{k}_2 = \Delta a \; \underline{f}(\underline{x})$$

$$\underline{x} = x_n + b_1 \underline{k}_1 + b_2 \underline{k}_2$$

$$\underline{k}_3 = \Delta a \underline{f}(\underline{x})$$

$$\underline{x} = \underline{x}_n + c_1 \underline{k}_1 + c_2 \underline{k}_2 + c_3 \underline{k}_3$$

$$\underline{k}_4 = \Delta a \underline{f}(x)$$

$$\underline{x} = \underline{x}_n + d_1 \underline{k}_1 + d_2 \underline{k}_2 + d_3 \underline{k}_3 + d_4 \underline{k}_4$$

The Runge-Kutta-Gill constants (ref. 2) are:

$a_1 = 1/2$ $\quad b_1 = (\sqrt{2}-1)/2$ $\quad b_2 = (2-\sqrt{2})/2$

$c_1 = 0$ $\quad c_2 = -\sqrt{2}/2$ $\quad c_3 = (2+\sqrt{2})/2$

$d_1 = 1/6$ $\quad d_2 = (2-\sqrt{2})/6$ $\quad d_3 = (2+\sqrt{2})/6$ $\quad d_4 = 1/6$

5.0 EXAMPLES

Tables I and II show examples of refraction corrections for

$N_o = 0.000395$

$H_S = 5446$ meters

$h_i = 0$ meters

$E_{Mi} = -0.239$ degrees

In tables I and II, $\Delta\rho = \rho_M - \rho$ meters and $\Delta E = E_{Mi} - E$ milliradians.

TABLE I.- SHORT- AND MEDIUM-RANGE REFRACTION CORRECTIONS

ρ_M, m	$\Delta\rho$, m	ΔE, mrad
100	0.0395	0.00 357
200	.0790	.00 721
300	.1185	.01 084
400	.1580	.01 448
500	.1975	.01 810
600	.2370	.02 173
700	.2765	.02 536
800	.3160	.02 899
900	.3555	.03 261
1000	.3950	.03 624
1 000	0.3950	0.03 624
2 000	.7903	.07 250
3 000	1.1859	.10 879
4 000	1.5817	.14 509
5 000	1.9779	.18 141
6 000	2.3743	.21 774
7 000	2.7711	.25 409
8 000	3.1680	.29 046
9 000	3.5653	.32 684
10 000	3.9628	.36 324

TABLE II.- LONG-RANGE REFRACTION CORRECTIONS

ρ_M, km	h_f, m	E_{Mf}, deg	$\Delta\rho$, m	ΔE, mrad
10	-37.5	-0.1909	3.9628	0.36 324
20	-66.6	-.1430	7.9512	.72 806
30	-87.4	-.0953	11.9606	1.09 418
40	-99.9	-.0478	15.9863	1.46 133
50	-104.1	-.0003	20.0236	1.82 923
60	-100.0	.0472	24.0678	2.19 759
70	-87.6	.0947	28.1141	2.56 615
80	-66.9	.1424	32.1577	2.93 461
90	-37.9	.1903	36.1938	3.30 271
100	-0.5	.2384	40.2176	3.67 015

6.0 REFERENCES

1. Bean, B. R.; Thayer, B. D.; and Cahoon, B. A.: Methods of Predicting the Atmospheric Bending of Radio Waves. National Bureau of Standards Report 6056, May 18, 1959.

2. Lear, William M.: Accuracy and Speed of 38 Self-Starting Integrators. JSC IN 78-FM-39, June 1978.